Articles

Total Alanine-Scanning Mutagenesis of Insulin-like Growth Factor I (IGF-I) Identifies Differential Binding Epitopes for IGFBP-1 and IGFBP-3

Yves Dubaquié and Henry B. Lowman*

Department of Protein Engineering, Genentech, Inc., 1 DNA Way, South San Francisco, California 94080

Received January 14, 1999; Revised Manuscript Received March 22, 1999

ABSTRACT: The bioavailability of insulin-like growth factor I (IGF-I) in the serum and tissues is controlled by members of the IGF binding protein family (IGFBP). These proteins form high-affinity complexes with IGF-I and thereby either inhibit or potentiate its mitogenic and metabolic effects. Thus, understanding the IGF−IGFBP interaction at the molecular level is crucial for attempts to modulate IGF-I activity in vivo. We have systematically investigated the binding contribution of each IGF-I amino acid side chain toward IGFBP-1 and IGFBP-3, combining alanine-scanning mutagenesis and monovalent phage display. Surprisingly, most IGF-I residues could be substituted by alanines, resulting in less than 5-fold affinity losses for IGFBP-3. In contrast, binding of IGFBP-1 was more sensitive to alanine substitutions in IGF-I. The glutamate and phenylalanine at positions 3 and 49 were identified as major specificity determinants for IGFBP-1: the corresponding alanine mutations, E3A and F49A, selectively decreased IGFBP-1 binding by 34- and 100-fold, whereas IGFBP-3 affinity was not affected or reduced maximally 4-fold. No side chain specificity determinant was found for IGFBP-3. Instead, our results suggest that the N-terminal backbone region of IGF-I is important for binding to IGFBP-3. The fact that the functional binding epitopes on IGF-I are overlapping but distinct for both binding proteins may be exploited to design binding protein-specific IGF variants.

The insulin-like growth factors I and II mediate multiple effects in vivo, including cell proliferation, cell differentiation, inhibition of cell death, and insulin-like activity (reviewed in refs *1* and *2*). Most of these mitogenic and metabolic responses are initiated by activation of the IGF-I[1] receptor, an $\alpha_2\beta_2$ heterotetramer closely related to the insulin receptor (*3, 4*). Both proteins are members of the tyrosine kinase receptor superfamily and share common intracellular signaling cascades (*2*). IGF−insulin hybrid receptors have been isolated, but their function is unknown. The IGF-I and insulin receptors bind their specific ligands with nanomolar affinity. IGF-I and insulin can cross-react with their respective noncognate receptors, albeit at a 100−1000-fold lower affinity (*2*). The crystal structure describing part of the extracellular portion of the IGF-I receptor has recently been reported (*5*).

Unlike insulin, the activity and half-life of IGF-I is modulated by six IGF-I binding proteins (IGFBP's 1−6) and perhaps additionally by a more distantly related class of proteins (*6*). IGFBP's can either inhibit or potentiate IGF activity, depending on whether they are soluble or cell membrane associated (*7*). The classical IGFBP's have a molecular mass ranging from 22 to 31 kDa and contain a total of 16−20 cysteines in their conserved amino- and carboxy-terminal domains (*7*−*9*). The central domain connecting both cysteine-rich regions is only weakly conserved and contains the cleavage sites for IGFBP-specific proteases (*9*−*11*). Further regulation of the IGFBP's may be achieved by phosphorylation and glycosylation (*7, 9*). There is no high-resolution structure available for any intact member of the IGFBP family. However, the NMR structures of two N-terminal fragments from IGFBP-5 which retain IGF-binding activity have recently been reported (*12*).

IGF-I is a single-chain 70 amino acid protein with high homology to proinsulin. Unlike the other members of the insulin superfamily, the C region of the IGF's is not proteolytically removed after translation. The solution NMR structures of IGF-I (*13, 14*), mini-IGF-I (an engineered variant lacking the C-chain; *15*), and IGF-II (*16, 17*) have been reported. It is generally accepted that distinct epitopes on IGF-I are used to bind receptor and binding proteins. While residues Y24, Y29, Y31, and Y60 are implicated in receptor binding, IGF mutants thereof still bind to IGFBP's (*18*−*21*). A multitude of mutagenesis studies have addressed the characterization of the IGFBP binding epitope on IGF-I (*22*−*27*). In summary, N-terminal residues 3 and 4 and the

* Corresponding author. Telephone: (650) 225-1171. Fax: (650) 225-3734. E-mail: hbl@gene.com.

[1] Abbreviations: ALS, acid-labile subunit of the IGF-I ternary complex; DTT, dithiothreitol; EDTA, ethylenediaminetetraacetic acid; HPLC, high-pressure liquid chromatography; IGF-I, insulin-like growth factor I; IGFBP, insulin-like growth factor binding protein; kDa, kilodalton; PBS, phosphate-buffered saline; PCR, polymerase chain reaction; SDS−PAGE, sodium dodecyl sulfate−polyacrylamide gel electrophoresis; TFA, trifluoroacetic acid.

10.1021/bi990089p CCC: $18.00
Published on Web 04/27/1999

helical region comprising residues 8−17 were found to be important for binding to the IGFBP's. Additionally, an epitope involving residues 49−51 in binding to IGFBP-1, -2, and -5 has been identified (*25*). Furthermore, a naturally ocurring truncated form of IGF-I lacking the first three N-terminal amino acids [called des(1−3)-IGF-I] was demonstrated to bind IGFBP-3 with 25 times lower affinity (*28*). In an attempt to characterize the binding contributions of exposed amino acid residues in the N-terminal helix, several alanine mutants of IGF-I were constructed (*29*). However, the circular dichroism spectra of these mutant proteins showed structural changes compared to wild-type IGF-I, making it difficult to clearly assign IGFBP binding contributions to the mutated side chains. A different approach was taken in a very recent study where the IGFBP-1 binding epitope on IGF-I was probed by heteronuclear NMR spectroscopy (*30*). The authors additionally identified residues R36, R37, and R50 to be functionally involved in binding to IGFBP-1.

Despite all these efforts, our view of the IGFBP binding epitope on IGF-I remains diffuse and at low resolution. The previous studies most often involved insertions of homologous insulin regions into IGF-I or protein truncations [e.g., des(1−3)-IGF-I]. Theoretically, these IGF-I variants can be either misfolded, lack energetically important side chains and polypeptide backbone contacts, or contain insulin residues that abolish IGFBP binding, for example, by charge repulsion or steric hindrance. It is difficult to differentiate between these effects in order to explain any observed affinity changes for the IGFBP's. Combining the results of all these earlier studies is further complicated by the fact that different techniques were used to analyze complex formation of the mutant IGF forms with the IGFBP's, ranging from radiolabeled ligand binding assays to biosensor analysis. To circumvent these problems, we have systematically probed the binding contribution of each IGF-I side chain toward IGFBP-1 and IGFBP-3 by alanine-scanning mutagenesis (*31, 32*). For practical reasons a phage display format was chosen, allowing for fast mutagenesis, isolation, and assay of IGF-I variants. The results obtained by phage ELISA yielded a high-resolution view of the respective functional binding epitopes for IGFBP-1 and IGFBP-3. Soluble mutants of interest were expressed, purified, and further characterized by biosensor analysis. The results of this study suggest that the binding epitopes for IGFBP-1 and IGFBP-3 are overlapping but distinct. Many more important side chain interactions were found for IGFBP-1 than for IGFBP-3, suggesting the involvement of the IGF-I backbone in binding to IGFBP-3. On the basis of our results the construction of binding protein-specific IGF mutants should be achievable. Such variants would be useful for testing the in vivo role of the binding proteins.

EXPERIMENTAL PROCEDURES

Construction of Phagemid Vector and Mutagenesis. The gene encoding mature human IGF-1 was amplified from pBKIGF2B (*33*) using PCR primers 5′-AGC TGC TTT GAT ATG CAT CTC CCG AAA CTC TGT GCG GT-3′ and 5′-GAG CGA TCT GGG TCT AGA CAG ATT TAG CGG GTT TCA G-3′. The resulting fragment was cut with *Nsi*I and *Xba*I and ligated into pH0753 previously digested with *Nsi*I and *Xba*I. pH0753 is a derivative of phGHam-g3 (*34*) in which the additional *Xba*I site in the alkaline phosphatase promoter (PhoA) region has been deleted using the oligonucleotide 5′-AAA AGG GTA TGT AGA GGT TGA GGT-3′. The ligated vector pH0753 containing the IGF-I open reading frame was named pIGF-g3. It encodes for IGF-I harboring the double mutation G1S-A70V fused to a fragment of the gene III protein (residues 249−406) from the *Escherichia coli* bacteriophage M13. This construct includes the *st*II signal sequence which directs the fusion protein to the periplasmic space of *E. coli* and allows monovalent display of the protein (*34*). Binding of G1S-A70V IGF-I to IGFBP-1 and -3 was found to be indistinguishable from wild-type IGF-I. Alanine mutagenesis was performed using single-stranded plasmid pIGF-g3 as template (*35*). All residues of IGF-I with the exception of cysteines and alanines were singly replaced by alanine. The resulting constructs were verified by DNA sequencing.

Binding of IGF Mutants Displayed on Phage to IGFBP-1 and -3 (Phage ELISA). Recombinant human IGFBP-1 and IGFBP-3 have previously been cloned and expressed in mammalian cells (*36*) and purified from conditioned media using an IGF affinity column (*37*). The recombinant material used here has been examined previously in studies of IGF-I binding and activity (*21, 38*).

Immunosorbent plates (Nunc, Maxisorp, 96 wells) were coated with 100 μL/well of 1 μg/mL IGFBP-1 or IGFBP-3 in PBS buffer, pH 7.2, at 4 °C overnight. The plates were then blocked with 0.5% Tween 20/PBS (also used as binding buffer) for 2 h at room temperature (proteinaceous blocking agents such as bovine serum albumin were avoided to prevent potential IGF or IGFBP contamination). *E. coli* cells (XL1-Blue, Stratagene) freshly transformed with phagemid vector were grown overnight in 5 mL of 2YT medium (*40*) in the presence of M13-VCS helper phage (Stratagene). Phage particles were harvested and resuspended in PBS buffer as described (*39*). Then phage concentrations were normalized to yield a maximal ELISA signal of 0.2−0.4 for each mutant (*39*). Threefold serial dilutions of soluble competitor were prepared in nonabsorbent microtiter plates (Nunc, F, 96 wells) with binding buffer (0.5% Tween 20/PBS) containing phage at the previously determined concentrations. The dilution range of competitor protein extended over 6 orders of magnitude, starting at 5 μM for IGFBP-1 and 500 nM for IGFBP-3. After blocking, the plates containing immobilized target were washed with 0.05% Tween 20/PBS buffer and subsequently incubated with 80 μL/well premixed phage−competitor solutions for 1 h at room temperature. After washing, bound phage was detected with 80 μL/well of a solution containing a primary rabbit anti-phage polyclonal antibody and a secondary goat anti-rabbit mAb horseradish peroxidase conjugate in 0.5% Tween 20/PBS. *o*-Phenylenediamine (Sigma) and tetramethylbenzidine (Kirkegaard and Perry) were used as chromogenic substrates, resulting in product detection at 492 and 450 nm, respectively. IC_{50} values were determined by fitting the binding data to a generic saturation curve (*39*). At least two individual clones of each IGF-I mutant were assayed. The numbers in Table 1 represent the mean ± standard deviation of individually assessed IC_{50} values.

Expression and Purification of Soluble IGF-I Mutants. Plasmid pBKIGF2B (*33*) expresses human wild-type IGF-I fused to the leader peptide of *lam*B under the control of the

Table 1: Apparent Affinities (IC_{50}) of IGF-I Variants for IGFBP-1 and IGFBP-3 Determined by Phage Display[a]

IGF-I mutant	IGFBP-1		IGFBP-3		relative specificity
	IC_{50} (nM)	relative IC_{50}	IC_{50} (nM)	relative IC_{50}	
S1A	5.2 ± 0.9	0.6 ± 0.1	0.91 ± 0.32	1.2 ± 0.4	0.5
P2A	11.0 ± 3.7	1.3 ± 0.5	0.81 ± 0.18	1.1 ± 0.2	1.2
E3A	278 ± 86	33.9 ± 10	1.05 ± 0.08	1.4 ± 0.1	24.2
T4A	19.4 ± 6.4	2.4 ± 0.8	0.80 ± 0.02	1.1 ± 0.03	2.2
L5A	55.3 ± 11.6	6.7 ± 1.4	1.53 ± 0.22	2.0 ± 0.3	3.3
G7A	>1000	>100	4.58 ± 0.28	6.1 ± 0.4	>16
E9A	8.6 ± 0.6	1.0 ± 0.1	1.32 ± 0.30	1.8 ± 0.4	0.6
L10A	311 ± 87	37.9 ± 11	3.55 ± 0.33	4.7 ± 0.4	8.1
V11A*	nd		nd		
D12A	4.3 ± 0.8	0.5 ± 0.1	1.49 ± 0.38	2.0 ± 0.5	0.3
L14A	36.7 ± 1.1	4.5 ± 0.1	0.90 ± 0.04	1.2 ± 0.1	3.7
Q15A	13.9 ± 0.9	1.7 ± 0.1	1.26 ± 0.41	1.7 ± 0.6	1.0
F16A	57.8 ± 20.1	7.0 ± 2.5	1.32 ± 0.25	1.8 ± 0.3	4.0
V17A	42.9 ± 3.2	5.2 ± 0.4	3.67 ± 1.02	4.9 ± 1.4	1.1
G19A	11.0 ± 2.3	1.3 ± 0.3	0.90 ± 0.28	1.2 ± 0.4	1.1
D20A	8.4 ± 4.1	1.0 ± 0.5	1.11 ± 0.06	1.5 ± 0.1	0.7
R21A	7.1 ± 1.6	0.9 ± 0.2	0.58 ± 0.01	0.8 ± 0.01	1.1
G22A	15.9 ± 2.8	1.9 ± 0.3	2.07 ± 0.11	2.8 ± 0.2	0.7
F23A	10.9 ± 1.9	1.3 ± 0.2	2.18 ± 0.01	2.9 ± 0.01	0.5
Y24A	13.3 ± 2.9	1.6 ± 0.4	2.53 ± 0.76	3.4 ± 1.0	0.5
F25A	181 ± 46	22.1 ± 5.6	3.69 ± 0.25	4.9 ± 0.3	4.5
N26A	9.1 ± 1.8	1.1 ± 0.2	0.90 ± 0.07	1.2 ± 0.1	0.9
K27A	12.8 ± 0.1	1.6 ± 0.01	0.66 ± 0.35	0.9 ± 0.5	1.8
P28A	9.3 ± 1.4	1.1 ± 0.2	1.41 ± 0.05	1.9 ± 0.1	0.6
T29A	7.3 ± 2.4	0.9 ± 0.3	1.23 ± 0.16	1.6 ± 0.2	0.5
G30A	7.1 ± 1.7	0.9 ± 0.2	0.58 ± 0.11	0.8 ± 0.2	1.1
Y31A	6.8 ± 0.5	0.8 ± 0.1	0.73 ± 0.10	1.0 ± 0.1	0.9
G32A	10.9 ± 1.3	1.3 ± 0.2	0.76 ± 0.28	1.0 ± 0.4	1.3
S33A	9.1 ± 1.0	1.1 ± 0.1	1.01 ± 0.24	1.3 ± 0.3	0.8
S34A	9.5 ± 0.7	1.2 ± 0.9	1.65 ± 0.21	2.2 ± 0.3	0.5
S35A	11.7 ± 0.6	1.4 ± 0.1	0.47 ± 0.01	0.6 ± 0.01	2.3
R36A*	nd		nd		
R37A	12.3 ± 0.1	1.5 ± 0.01	0.75 ± 0.08	1.00 ± 0.1	1.5
P39A*	nd		nd		
Q40A	10.2 ± 0.9	1.2 ± 0.1	0.56 ± 0.03	0.7 ± 0.04	1.7
T41A	13.7 ± 3.1	1.7 ± 0.4	0.43 ± 0.06	0.6 ± 0.1	2.9
G42A	15.7 ± 3.4	1.9 ± 0.4	0.53 ± 0.20	0.7 ± 0.3	2.7
I43A	31.3 ± 4.1	3.8 ± 0.5	1.17 ± 0.07	1.6 ± 0.1	2.4
V44A	18.8 ± 5.4	2.3 ± 0.7	1.03 ± 0.06	1.4 ± 0.1	1.7
D45A	4.7 ± 0.7	0.6 ± 0.1	0.69 ± 0.21	0.9 ± 0.3	0.6
E46A	7.9 ± 2.1	1.0 ± 0.3	0.94 ± 0.28	1.3 ± 0.4	0.8
F49A	>1000	>100	2.72 ± 1.11	3.6 ± 1.5	>28
R50A	16.2 ± 1.8	2.0 ± 0.2	0.64 ± 0.18	0.9 ± 0.2	2.3
S51A	13.4 ± 0.4	1.6 ± 0.1	0.65 ± 0.35	0.9 ± 0.5	1.9
D53A	15.3 ± 2.8	1.9 ± 0.3	1.05 ± 0.11	1.2 ± 0.3	1.6
L54A	23.1 ± 12.0	2.8 ± 1.5	1.83 ± 0.91	2.4 ± 1.2	1.2
R55A	9.0 ± 2.3	1.1 ± 0.3	0.66 ± 0.03	0.9 ± 0.04	1.2
R56A	13.1 ± 1.8	1.6 ± 0.2	1.00 ± 0.19	1.3 ± 0.3	1.2
L57A	21.8 ± 5.6	2.7 ± 0.7	1.78 ± 0.56	2.4 ± 0.8	1.1
E58A	11.9 ± 1.8	1.5 ± 0.2	1.03 ± 0.47	1.4 ± 0.6	1.1
M59A	13.1 ± 1.8	1.6 ± 0.2	0.74 ± 0.14	1.0 ± 0.2	1.6
Y60A	6.6 ± 1.8	0.8 ± 0.2	0.52 ± 0.01	0.7 ± 0.01	1.2
P63A	>1000	>100	>100	>100	
L64A	12.1 ± 3.3	1.5 ± 0.4	0.93 ± 0.03	1.2 ± 0.04	1.2
K65A	12.4 ± 0.6	1.5 ± 0.1	0.69 ± 0.05	0.9 ± 0.1	1.6
P66A	9.4 ± 3.2	1.1 ± 0.4	0.57 ± 0.12	0.8 ± 0.2	1.5
K68A	10.5 ± 2.8	1.3 ± 0.3	0.76 ± 0.23	1.0 ± 0.3	1.3
S69A	12.8 ± 2.3	1.6 ± 0.3	0.71 ± 0.62	1.2 ± 0.5	1.3
V70A	19.1 ± 0.7	2.3 ± 0.1	0.68 ± 0.15	0.9 ± 0.2	2.6
S1G	11.2 ± 1.1	1.4 ± 0.1	0.99 ± 0.42	1.3 ± 0.6	1.0
IGF-I WT	8.4 ± 0.8	1.0 ± 0.1	1.01 ± 0.42	1.3 ± 0.6	0.8
G1S-A70V	8.2 ± 1.6	1.0 ± 0.2	0.75 ± 0.32	1.0 ± 0.4	1.0
Ala(1−3)-IGF	90.4 ± 9.6	11.0 ± 1.2	1.12 ± 0.04	1.5 ± 0.05	7.3
des(1−2)-IGF	5.0 ± 0.1	0.6 ± 0.02	0.53 ± 0.03	0.7 ± 0.04	0.9

[a] IC_{50} values for each mutant were determined by phage ELISA as shown in Figure 1. The variants denoted with an asterisk were not successfully displayed on phage (nd), as judged by antibody experiments (see Results section for details). Relative IC_{50} is defined as $IC_{50\ mut}/IC_{50\ G1S-A70V}$. Relative specificity is defined as relative $IC_{50\ IGFBP-1}$/relative $IC_{50\ IGFBP-3}$ for each variant. Values are the mean ± SD, $n \geq 2$.

P_{pho}A promotor. For ease of site-directed mutagenesis the phage f1 origin of replication (f1 ori) was introduced into plasmid pBKIGF2B. For that purpose a 466 bp *Bam*HI fragment containing the f1 ori was excised from pH0753

Table 2: Kinetic Parameters for the Interaction of Purified IGF-I Mutants with IGFBP-1 and IGFBP-3 Determined by BIAcore Analysis

	binding to IGFBP-1				
	k_a ($\times 10^4$ M^{-1} s^{-1})	k_d ($\times 10^{-4}$ s^{-1})	K_D (nM)	relative K_D[a]	relative IC_{50}[a]
IGF-I WT	3.2 ± 0.2	4.1 ± 0.2	13.0 ± 1.0	1.0	1.0
G1S-A70V	3.2 ± 0.2	4.5 ± 0.01	14.0 ± 0.7	1.1	1.0
T4A	1.9 ± 0.2	16.7 ± 1.6	90.0 ± 11.0	6.9	2.4
V11A	1.9 ± 0.1	12.3 ± 0.6	66.5 ± 4.5	5.1	
F16A	1.9 ± 0.6	60.3 ± 4.5	321 ± 98	25	6.0
F25A	1.5 ± 0.5	49.0 ± 5.7	323 ± 107	25	22
R36A	4.0 ± 0.2	5.6 ± 0.2	13.9 ± 0.8	1.1	
P39A	3.1 ± 0.2	4.2 ± 0.1	13.6 ± 0.8	1.0	
F49A	1.3 ± 0.8	115 ± 1.5	913 ± 551	70	>100
P63A	3.0 ± 0.4	3.5 ± 0.2	11.7 ± 1.8	0.9	>100
	binding to IGFBP-3				
	k_a ($\times 10^5$ M^{-1} s^{-1})	k_d ($\times 10^{-4}$ s^{-1})	K_D (nM)	relative K_D[a]	relative IC_{50}[a]
IGF-I WT	3.2 ± 0.5	4.7 ± 0.8	1.5 ± 0.3	1	1.4
G1S-A70V	2.9 ± 0.8	6.3 ± 0.5	2.2 ± 0.6	1.5	1
T4A	1.8 ± 0.6	5.5 ± 0.1	3.1 ± 1.0	2.1	1.1
V11A	3.1 ± 0.5	20.9 ± 2.8	6.7 ± 1.3	4.5	
F16A	1.1 ± 0.4	11.4 ± 2.7	10.3 ± 4.7	6.9	1.8
F25A	1.5 ± 0.1	11.8 ± 0.1	7.7 ± 0.3	5.1	4.9
R36A	4.0 ± 0.1	4.7 ± 0.2	1.2 ± 0.1	0.8	
P39A	2.7 ± 0.2	6.0 ± 0.3	2.2 ± 0.2	1.5	
F49A	2.7 ± 0.7	17.1 ± 0.9	6.3 ± 1.7	4.2	3.6
P63A	3.1 ± 0.5	3.9 ± 0.3	1.3 ± 0.3	0.9	>100

[a] The relative changes in dissociation constants ($K_{D\ mut}/K_{D\ wt}$) are compared to the relative IC_{50} values ($IC_{50\ mut}/IC_{50\ G1S\text{-}A70V}$) determined by phage display (Table 1).

(*34*) while plasmid pBKIGF2B was linearized with *Eco*RI. The vector and fragment were both treated with Klenow enzyme to fill in restriction site overhangs prior to blunt-end ligation. Correct constructs were selected for the ability to produce single-stranded phagemid DNA in the presence of M13VCS helper phage. The resulting phagemid vector was named pBKIGF2B-f1-ori and was used as a template to construct the IGF-I Ala mutants of interest (see Table 2) using the procedure of Kunkel et al. (*35*). Every mutagenesis step was confirmed by DNA sequencing.

Expression of IGF-I mutants was as described for the IGF-I wild type (*41*) but without transient overexpression of oxidoreductases. The purification procedure was based on a previous protocol (*42*) with minor adaptations. Typically, 6 g of wet cell paste (equivalent to 2 L of low phosphate medium grown for 24 h) was resuspended in 150 mL of 25 mM Tris-HCl, pH 7.5, containing 5 mM EDTA. Cells were lysed in a microfluidizer (Microfluidics Corp., Newton, MA), and refractile particles containing accumulated IGF-I aggregates were collected by centrifugation at 12000*g*. Refractile particles were washed twice with lysis buffer, twice with lysis buffer containing 1% *N*-lauroylsarcosine (Sigma) in order to extract membrane proteins, and twice with lysis buffer again. Washed refractile bodies were resuspended at approximately 2 mg/mL in 50 mM CAPS [3-(cyclohexylamino)-1-propanesulfonic acid; Sigma] buffer, pH 10.4, containing 2 M urea, 100 mM NaCl, 20% MeOH, and 2 mM DTT. This procedure combines solubilization of refractile bodies and subsequent oxidative refolding of IGF-I mutants (*42*). After 3 h at room temperature the refolding solutions were filtered through microconcentrator membranes (Centricon, Amicon) with a molecular mass cutoff of 50 kDa. The majority of monomeric IGF-I is recovered in the eluate, while higher molecular weight contaminants are concentrated in the retentate. At this point IGF-I fractions were >95% pure, as judged from SDS−PAGE analysis. To separate correctly disulfide-bonded IGF-I from IGF swap (containing two non-native disulfides; *43, 44*) refolding solutions were acidified with 5% acetic acid and loaded on a Dynamax C18 semipreparative HPLC column (Varian; 10.0 mm i.d.) at 4 mL/min. Buffers were H_2O/0.1% TFA (A) and acetonitrile/0.1% TFA (B). Separation of the disulfide isomers was achieved by applying the following gradient: 0−30% bufferB in 20 min and 30−45% buffer B in 60 min. IGF swap and correctly folded IGF-I eluted in two distinct peaks with baseline separation. The identity of the eluted IGF-I mutants was verified by mass spectrometry of each HPLC peak, which also confirmed homogeneity of the samples. The material of both peaks was assayed for binding to IGFBP-1 and IGFBP-3 in order to identify the peak containing IGF-I with the correct disulfide linkages. The incorrect disulfide isomer always eluted earlier than the correctly folded form, and the ratio was approximately 1:2 for all tested variants. After HPLC purification, samples were lyophilized and reconstituted at approximately 1 mg/mL in 100 mM HEPES buffer, pH 7.4. Specific protein concentration was assessed by the BCA method (Pierce) using a wild-type IGF-I standard previously determined by quantitative amino acid analysis.

Biosensor Kinetic Measurements. The binding affinities of the IGF variants for IGFBP-1 and IGFBP-3 were determined using a BIAcore-2000 real time kinetic interaction analysis system (Biacore, Inc., Piscataway, NJ) to measure association (k_a) and dissociation (k_d) rates. Carboxymethylated Dextran biosensor chips (CM5, BIAcore Inc.) were activated with EDC [*N*-ethyl-*N*′-(3-dimethylaminopropyl)carbodiimide hydrochloride] and NHS (*N*-hydroxysuccinimide) according to the supplier's instructions. For immobilization, IGF mutants in 20 mM sodium acetate, pH 4.8, were injected onto the biosensor chip at a concentration of 50 μg/mL to yield approximately 450−600 RU's (resonance responce units) of covalently coupled protein. Unreacted groups were blocked with an injection of 1 M

ethanolamine. Kinetic measurements were carried out by injecting 2-fold serial dilutions (starting at 1 μM) of either IGFBP-1 or IGFBP-3 in running buffer (PBS, 0.05% Tween 20, 0.1% ovalbumin, 0.01% sodium azide) at 25 °C using a flow rate of 20 μL/min. Association rates (k_a) and dissociation rates (k_d) were calculated separately using a 1:1 Langmuir association model in the BIAcore evaluation software version 3.0. The equilibrium dissociation constant (K_D) was calculated as k_d/k_a.

RESULTS

Monovalent Phage Display of IGF-I. To perform a rapid and comprehensive alanine scan of the 70 amino acid residues of IGF-I, we first tested whether the protein could be monovalently displayed on the surface of phage M13 (*45*). Phage display technology combines the advantage of rapid single-stranded DNA mutagenesis with an easy purification of the resulting mutant protein, simply by isolation of the corresponding phage particles (e.g., *46*). For cloning purposes the first and the last amino acids of IGF-I were changed from Gly to Ser and from Ala to Val, respectively (termed IGF-I G1S-A70V). When phage particles displaying IGF-I G1S-A70V were isolated and assayed in a binding competition phage ELISA for their affinity to IGFBP's, the half-maximal inhibitory concentrations (IC_{50}) determined in that experiment were 8.5 nM for IGFBP-1 and 0.5 nM for IGFBP-3 (Figure 1). These values are in good agreement with dissociation constants determined by BIAcore experiments using wild-type IGF-I (this study; *28*). Wild-type IGF-I affinities determined by radioactive immunoassays (RIA) are ~2.8 nM for IGFBP-1 and ~0.8 nM for IGFBP-3 (P. Fielder, personal communication), further supporting our IC_{50} values derived from phage ELISA. Additionally, phage particles displaying IGF-I G1S-A70V were efficiently captured by 11 independent monoclonal mouse anti-IGF-I antibodies immobilized on microtiter plates (data not shown). These results together suggested that the displayed IGF variant is folded correctly and accessible on the surface of the phage particles.

Ala-Scanning Mutagenesis of IGF-I Binding to IGFBP-1 and IGFBP-3. All residues of IGF-I G1S-A70V with the exception of the four native alanines and six cysteines were singly substituted by alanine, using the described IGF-I G1S-A70V gIII vector as a template. Additionally, the single mutants S1G and V70A and the double mutation restoring wild-type IGF-I were constructed. Each of these constructs was expressed in *E. coli* and displayed on phage. IC_{50} values for binding to IGFBP-1 and IGFBP-3 were determined by competitive phage ELISA as shown in Figure 1. At least two different clones of every mutant were tested. The resulting IC_{50} values are listed in Table 1, and the loss or gain in IC_{50} for each mutant with respect to G1S-A70V is graphed in Figure 2.

The majority of the Ala mutants yielded only minor changes in IC_{50} values in the phage ELISA. Importantly, wild-type IGF-I showed the same affinities for IGFBP-1 and IGFBP-3 as G1S-A70V in which background the alanine substitutions were perfomed (Table 1, Figure 2). Only a few residues caused considerable (>10-fold) losses in affinity when changed to alanine: E3, G7, L10, V11, F25, R36, P39, F49, and P63 for IGFBP-1 binding; V11, R36, P39, and P63 for IGFBP-3 binding. To probe whether Ala substitutions

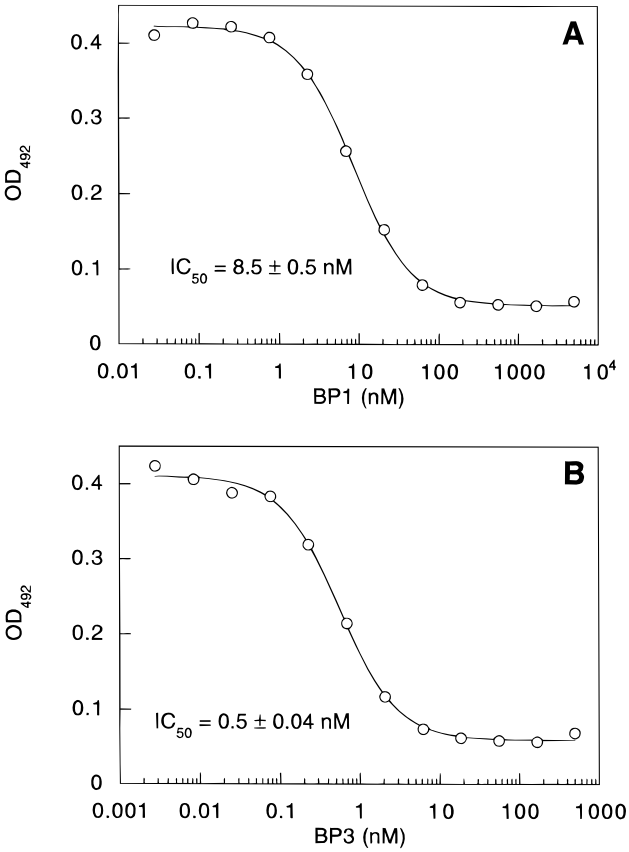

FIGURE 1: Phage ELISA of G1S-A70V IGF-I binding to IGFBP-1 and IGFBP-3. Microtiter plates coated with 1 μg/mL IGFBP-1 (A) or IGFBP-3 (B) were incubated with phage particles displaying G1S-A70V in the presence of the indicated amounts of soluble competitor protein, IGFBP-1 (A) or IGFBP-3 (B). The inhibitory concentration (IC_{50}) of competitor which resulted in half-maximal binding of the phagemid in that particular experiment is denoted for the respective IGFBP.

caused negative effects on the structure or the expression of the displayed variants, we tested whether the mutants showing >10-fold loss of affinity for both IGFBP's (V11A, R36A, P39A, P63A) were recognized by a collection of monoclonal antibodies raised against wild-type IGF-I. Of these tested variants V11A, R36A, and P39A were not recognized at all by the antibodies or gave only poor ELISA signals (data not shown). This result indicates that these three mutants are either partially unfolded or not displayed on phage, due to lack of expression or packaging into phage particles. The fact that P63A is recognized by the majority of our antibodies demonstrates that this variant is displayed. However, it does not rule out the possibility that the structure of this variant undergoes local perturbations, since we do not know to which exact locations our antibodies map on the structure of IGF-I. Furthermore, it has been noted that Ala substitutions of glycines and prolines can lead to structural perturbations of the protein backbone (*47*; see also Discussion).

We found only a few modest improvements in binding affinity by alanine replacements. S1A, D12A, and D45A showed an approximately 2-fold increase in IGFBP-1 binding, while S35A and T41A showed a similar effect for IGFBP-3. However, 2-fold changes in IC_{50} values are at the limit of precision in these experiments.

IGFBP Specificity Determinants. E3A, G7A, L10A, F25A, and F49A show a differential effect in binding IGFBP-1

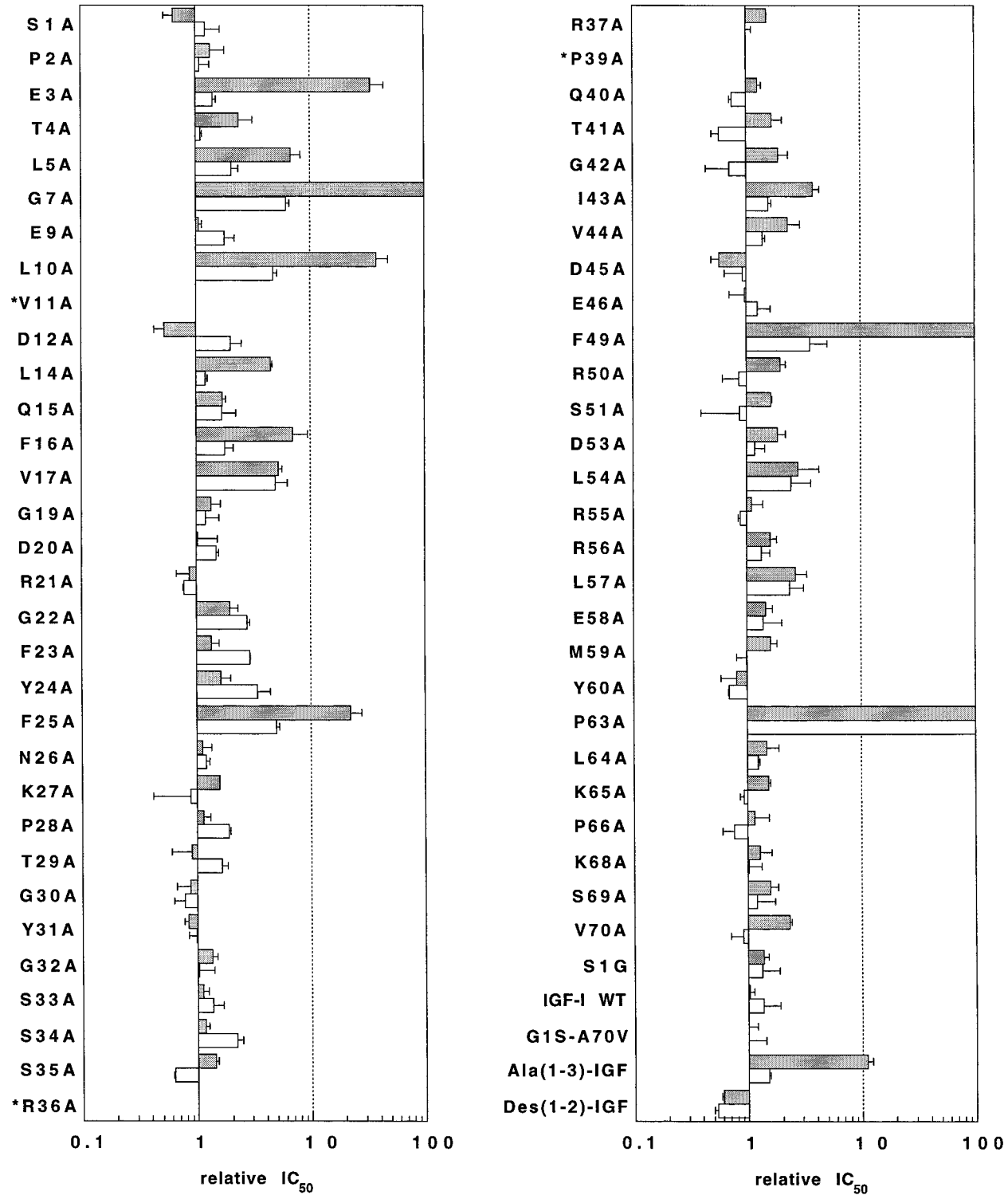

FIGURE 2: Loss or gain of IGFBP affinity for the IGF-I mutants tested by phage ELISA. Relative IC_{50} values ($IC_{50\,mut}/IC_{50\,G1S-A70V}$) of each IGF-I mutant are shown for IGFBP-1 (filled bars) and IGFBP-3 (open bars). Data are taken from Table 1. Relative IC_{50} values <1 denote gain of affinity; values >1 denote loss of affinity. The asterisks indicate that these particular variants were not displayed on phage, as judged by antibody binding.

versus IGFBP-3. For these five IGF-I single Ala mutants the relative IC_{50} for IGFBP-1 differs by more than 4-fold from the one for IGFBP-3 (Figure 2; Table 1, relative specificity). E3A and F49A show the biggest relative specificity factors in this group. Alanine substitution of E3 has virtually no effect on IGFBP-3 affinity (1.4-fold) while binding to IGFBP-1 is weakened 34-fold. Even more dramatic, the affinity of F49A is down more than 100-fold for IGFBP-1 but only 3.6-fold for BP-3. This result is illustrated in a direct comparison by phage ELISA. Phage particles displaying IGF-I F49A were added to IGFBP-3 coated wells in the presence of soluble IGFBP-1 (Figure 3A) or IGFBP-3 (Figure 3B). Compared to control phage displaying IGF-I G1S-A70V, the binding curve of F49A shifts by more than 2 orders of magnitude in the IGFBP-1 competition (Figure 3A). In contrast, the binding curves are

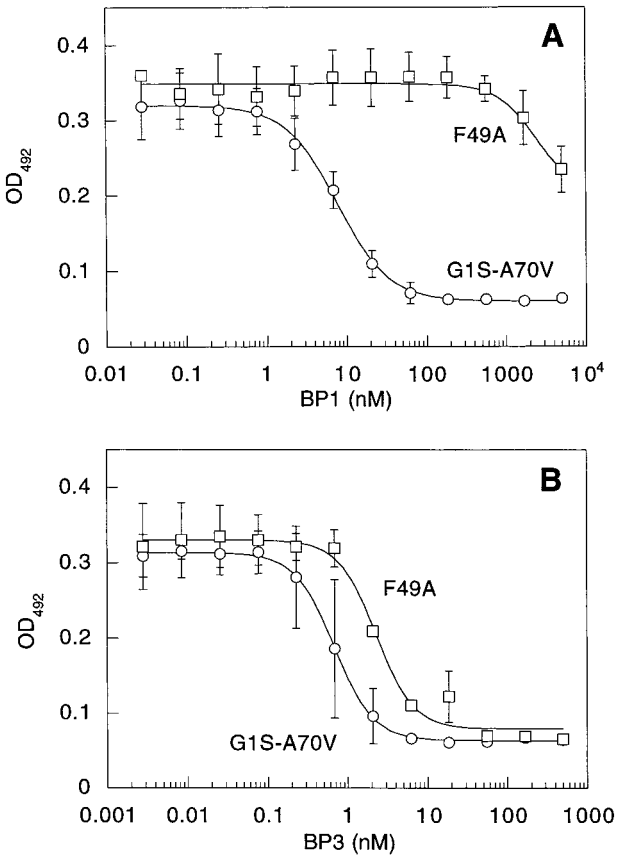

FIGURE 3: Binding specificity of the IGF-I variant F49A displayed on phage. Phagemid particles displaying F49A (□) were bound to plates coated with IGFBP-3 in the presence of the indicated amounts of soluble IGFBP-1 (A) or IGFBP-3 (B). The same experiment was carried out in parallel with phage displaying the wild-type-like IGF-I variant G1S-A70V (○). See Tables 1 and 2 for absolute IC_{50} values. Data points are the mean ± SD, $n = 2$.

similar in the IGFBP-3 competition, and the IC_{50} values differ by less than a factor of 4 (Figure 3B). Thus, E3 and F49 are two major specificity determinants for IGFBP-1 binding in the IGF-I molecule.

Residues G7, L10, and F25 seem to be important for binding of both IGFBP's, although showing a more pronounced loss of affinity for IGFBP-1 than for IGFBP-3 when substituted by alanines. We did not identify any significant specificity determinant for IGFBP-3, such as a mutant binding much tighter to IGFBP-1 than to IGFBP-3. However, mutations E9A, D12A, F23A, Y24A, T29A, S34A, and D45A had slightly larger (about 2-fold) effects on IGFBP-3 than on IGFBP-1 binding.

BIAcore Measurements of Purified Soluble IGF Mutants. To validate the results obtained by phage ELISA, we expressed and purified specific alanine mutants for kinetic analysis using a BIAcore instrument. The dissociation constant (K_D) of wild-type IGF-I was determined to be 13 nM for IGFBP-1 and 1.5 nM for IGFBP-3 (Figure 4A,B; Table 2). The difference in affinity for the IGFBP's is due to a 10-fold faster association rate (k_a) of IGF-I to IGFBP-3 (3.2×10^5 versus 3.2×10^4 M^{-1} s^{-1}). These results correspond well with the absolute IC_{50} values determined by phage ELISA (Figure 1A,B; Table 1). As expected, the double mutant G1S-A70V showed kinetic parameters essentially indistinguishable from wild type (Table 2).

V11A, R36A, and P39A were tested because these variants had not been displayed correctly on phage, based upon the antibody recognition experiments (see above). R36A and P39A showed wild-type kinetics for both binding proteins, whereas V11A showed a 5-fold reduction in affinity for both IGFBP-1 and IGFBP-3.

Furthermore, we decided to examine the soluble IGF variant T4A. This residue had been implicated in IGFBP binding in earlier publications (*22*, *24*) but had shown modest effects in our phage assays. The increase in the K_D values of T4A relative to wild-type IGF-I is approximately 2−3-fold higher than the IC_{50} ratios determined by phage ELISA (Table 2). A bigger discrepancy between the results obtained by phage and the biosensor analysis is seen for F16A. In this case the two methods differ by a factor of 4. It has been shown that mutations in the first α-helical region have a destabilizing effect on the IGF−protein structure (*29*). We postulate that the g3 fusion protein on the surface of the phage might be more stable than the refolded, purified soluble protein (see also Discussion). This is supported by the BIAcore results obtained for F25A and F49A, two residues located outside the structurally sensitive N-terminal helix. The respective changes in K_D and IC_{50} values are in excellent agreement for these two mutants (Table 2). The differential effect of F49A on binding to the IGFBP's was confirmed by the BIAcore analysis. A 70-fold decrease in affinity was measured for IGFBP-1 binding (Figure 4C; Table 2) whereas IGFBP-3 binding was reduced only 4-fold (Figure 4D; Table 2).

The binding kinetics for soluble P63A were identical to those for wild-type IGF-I (Table 2). This is in contrast to the data obtained on phage, where IGFBP binding was not detectable despite successful display of P63A as judged by antibody binding (Table 1; see Discussion).

Role of the N-Terminal IGF-I Residues. Surprisingly, the IGFBP-3 interaction was generally much less affected by the Ala substitutions than was the interaction with IGFBP-1, despite the fact that IGFBP-3 binds IGF-I with approximately 10-fold higher affinity. Apart from P63A, no alanine mutant exhibited a >6-fold reduction in IGFBP-3 affinity (Figure 2; Table 1). What determinants on IGF-I are responsible for the high-affinity binding to IGFBP-3? It had previously been shown in biosensor experiments that des-(1−3)-IGF-I binds IGFBP-3 with 25-fold reduced affinity (*28*). This naturally occurring form of IGF-I lacks the first three N-terminal residues and shows increased mitogenic potency, presumably due to its reduction in IGFBP binding (*23*). Since none of the first three amino acid side chains seem to contribute any energy to the binding of IGFBP-3 (Table 1) but nevertheless des(1−3)-IGF-I is compromised in IGFBP-3 binding, we hypothesized that backbone interactions might be involved. To test this hypothesis, we displayed on phage a triple alanine mutant [Ala(1−3)-IGF-I], substituting the first three N-terminal amino acids. If the backbone in that region contributes to the interaction with IGFBP-3, this mutant should be able to bind. Binding to IGFBP-1, however, should be reduced due to the lack of the E3 side chain (Table 1). As a control we generated the des(1−2)-IGF-I mutant, testing for any potential backbone interactions with IGFBP-1 at positions 1 and 2. As expected, Ala(1−3)-IGF-I showed a decreased IGFBP-1 affinity similar to that of E3A but no change in IGFBP-3 affinity (Table 1; Figure

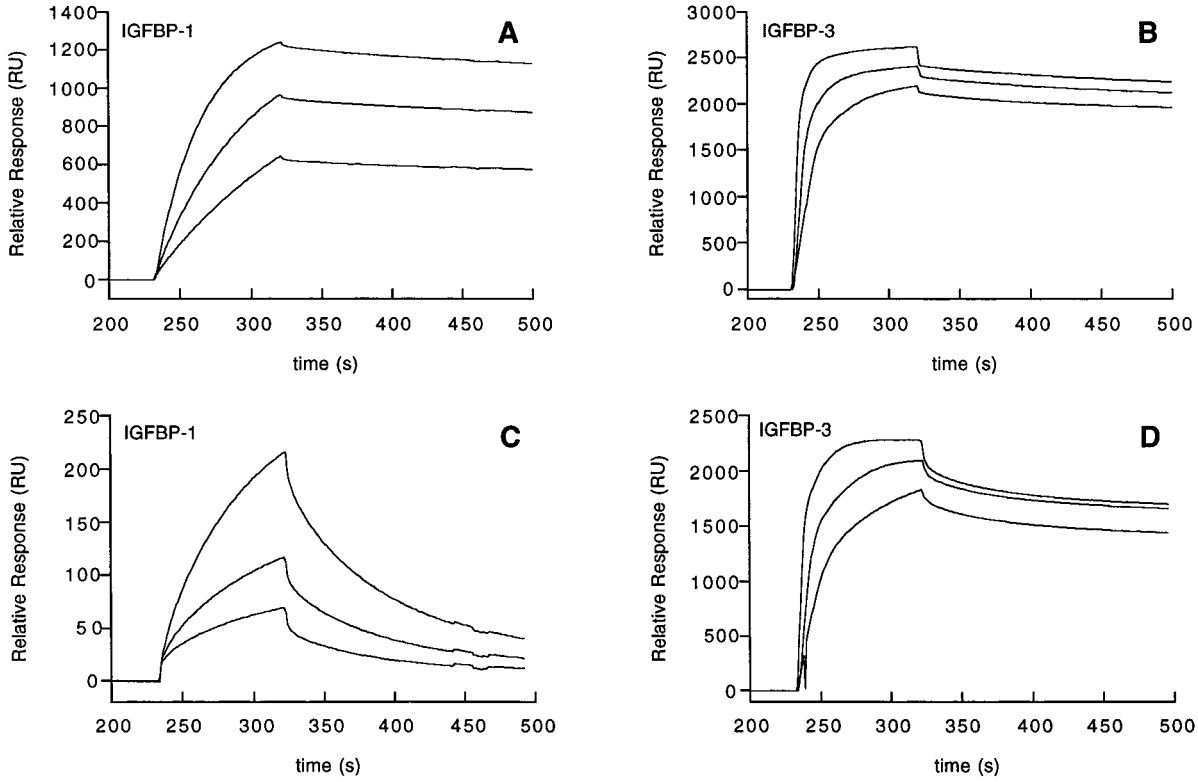

FIGURE 4: Biosensor analysis of IGFBP binding to immobilized IGF-I variants. Sensorgrams are shown for IGFBP-1 (A, C) or IGFBP-3 (B, D) binding to immobilized wild-type IGF-I (A, B) or F49A (C, D). The concentrations of ligand in each experiment were 1 μM, 500 nM, and 250 nM. See Table 2 for kinetic parameters.

2). For des(1−2)-IGF-I, no difference in affinity was observed for both binding proteins. Combined with the observations on des(1−3)-IGF-I (*28*), these results suggest that the peptide backbone between residues 3 and 4 of IGF-I mediates important interactions with IGFBP-3.

DISCUSSION

We have probed the functional IGFBP-1 and IGFBP-3 binding epitopes on the surface of IGF-I by alanine-scanning mutagenesis. Both binding epitopes are illustrated in Figure 5. Individual IGF-I side chain interactions play a much more important role for binding to IGFBP-1 than to IGFBP-3. Two major binding patches are found for IGFBP-1 (Figure 5A). One is situated on the upper face of the N-terminal helix (composed of G7, L10, V11, L14, F25, I43, and V44) and one on the lower face (composed of E3, T4, L5, F16, V17, and L54). These two binding patches are bridged by F49 and R50. For IGFBP-3, the binding epitope is more diffuse and has shifted to include G22, F23, and Y24 (Figure 5B). Binding of IGFBP-3 is generally much less sensitive to alanine substitutions. In fact, the biggest reduction in affinity (apart fom P63A, see below) is a 6-fold decrease seen for G7A. This result is intriguing since IGFBP-3 binds with 10-fold higher affinity to IGF-I than does IGFBP-1. Most probably, interactions originating from the IGF-I main chain backbone are contributing to the binding of IGFBP-3. This hypothesis is further substantiated by our experiments with the Ala(1−3)-IGF mutant. While the single and triple alanine substitutions have no effect on IGFBP-3 binding, deletion of the first three amino acids results in a 25-fold decrease in affinity (*23*, *25*, *28*). In summary, IGF-I uses different binding modes to associate with IGFBP-1 and IGFBP-3: a few amino acid side chain interactions are important for binding to IGFBP-1, while backbone interactions seem to play a major energetic role for binding to IGFBP-3.

A recent publication has investigated the binding epitope on IGF-I for IGFBP-1 by heteronuclear NMR spectroscopy (*30*). The authors found that IGF-I residues 29, 30, 36, 37, 40, 41, 63, 65, and 66 among others experienced chemical shift perturbations upon complexation with IGFBP-1 at 30 °C. Furthermore, Jansson and co-workers (*30*) identified R36, R37, and R50 to be part of the functional binding epitope and tested those alanine mutants in BIAcore experiments. The largest change in affinity observed by these authors, however, was a 3-fold decrease for R50A. This is a very small effect, corresponding to a change in free energy of binding ($\Delta\Delta G$) of about 0.7 kcal/mol. The typical error in these experiments is ∼0.5 kcal/mol (*48*). Our phage display data agree well with this result, since we found a 2.4-fold decrease in IC_{50} for the IGF-I variant R50A (Table 1). This residue is adjacent to F49, which is one of the side chains that contributes a major part of the IGFBP-1 binding energy ($\Delta\Delta G \cong 2.6$ kcal/mol). Unfortunately, due to the structural flexibility of IGF-I already observed in the first NMR study of the hormone (*13*), Jansson et al. (*30*) were unable to completely assign many residues in the NMR spectrum, including F49. On the basis of our results regarding the binding epitope differences, it would be interesting to see what main chain interactions might be revealed in an NMR study of IGFBP-3 in complex with IGF-I.

In similar studies of protein−protein interfaces it was found that only a few side chain residues contribute to the bulk of free binding energy (*49*, *50*). The same holds true for the IGF−IGFBP-1 interaction. However, here, as was

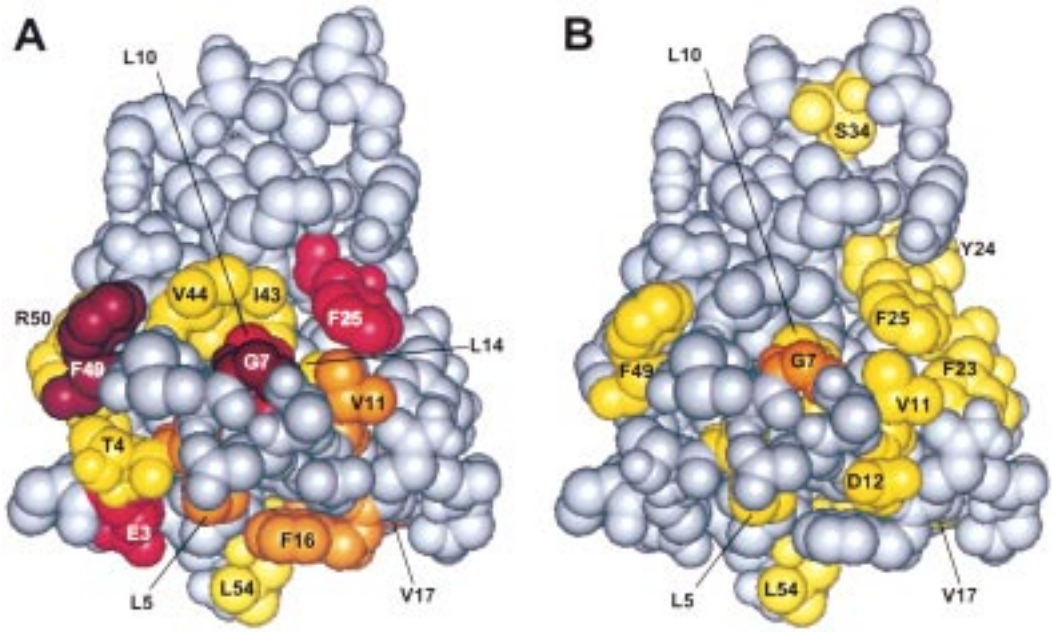

FIGURE 5: Model of the functional binding epitopes for IGFBP-1 and IGFBP-3 on the surface of IGF-I. Amino acid side chains were classified according to their relative contribution in binding energy (Table 1) and colored as follows: no effect (gray); 2−5-fold loss of apparent affinity (yellow); 5−10-fold (orange); 10−100-fold (bright red); >100-fold (dark red). If available, numbers from phage ELISA experiments in Table 1 were used. BIAcore data were used instead for V11A, R36A, P39A, and P63A (Table 2). The NMR structure of IGF-I (*13*) was represented using the program Insight II (MSI, San Diego, CA). The binding epitope for IGFBP-1 (A) is located on the "upper" and "lower" face of the N-terminal helix (residues 8−17), connected by the energetically important residue F49. For IGFBP-3 (B), individual IGF-I side chains contribute very little binding energy. The binding epitope has shifted away from the N-terminus and newly includes G22, F23, and Y24. Additionally, IGF-I polypeptide backbone interactions may play a more important role for binding IGFBP-3 than IGFBP-1 (see text for details).

noticed for tissue factor binding to factor VIIa, the magnitude of the $\Delta\Delta G$ values derived from important side chains is smaller than in the case of growth hormone (*50*). The residues with predominant $\Delta\Delta$G contributions are not clustered on the IGF-I surface as in the growth hormone−receptor interface (*49*) but still form a continuous IGFBP-1 binding epitope (Figure 5A). In contrast, the IGFBP-3 binding epitope on IGF-I is discontinuous, and side chains contribute very modest individual binding energies. Clearly, the explanation of these differences awaits further functional characterization of the complementary binding epitopes on IGFBP-1 and IGFBP-3.

The results obtained in this study by phage display agree well with published observations of IGFBP binding. For example, it was noted by Clemmons and co-workers that Y31A IGF showed a 2-fold increase in IC_{50} for IGFBP-1 (*25*). We find the same in our phage display format (Table 1). Similarly, alanine substitution of D12 was shown by BIAcore analysis to increase IGFBP-1 affinity 2-fold (*29*). Again the phage display results agree perfectly. Only two major discrepancies between IC_{50} ratios obtained by phage ELISA and BIAcore results were observed, namely, for F16A and P63A (see Table 2). It has been shown that substitution of residue F16 by alanine induces structural changes in the IGF-I molecule, leading to a decrease in IGFBP affinity (*29*). We noticed the same effect in our BIAcore results, but the affinity decrease was less pronounced in our phage ELISA's. Both BIAcore measurements used IGF F16A that had been refolded during the purification procedure (*29*; see Experimental Procedures). In phage display, however, the protein of interest is translocated naturally by the secretion machinery of *E. coli*, and the low abundance of the expressed heterologous protein in monovalent phage display (<1 molecule per phage particle) may disfavor aggregation and misfolding. Fusion of IGF-I to the truncated g3 phage protein might exert an additional stabilizing effect on the native structure of the polypeptide. For P63A, we postulate that the reasons for lack of observable IGFBP-1 or -3 binding are low display levels of P63A on the surface of phage. The mutation might decrease display levels to such an extent that antibody recognition is still possible while IGFBP binding is not detectable. The essentially wild-type-like binding of P63A is supported by the following independent observations: (a) residue P63 is located on the opposite side of the IGF-I molecule with respect to the main binding epitope; (b) Jansson et al. (*30*) concluded that the C-terminal part of IGF-I is not involved in direct IGFBP-1 contacts but rather undergoes indirect conformational changes upon complex formation; (c) binding of IGFBP-1 or -3 to IGF-I was not inhibited by antibodies recognizing the C-terminal D-domain of IGF-I (*51*). These findings further support earlier observations that the D-domain, which begins at residue P63, is not involved in binding of IGFBP-1 or -3 (*22*).

The majority of IGF-I in the circulation is found in complex with IGFBP-3 and a third protein termed the acid-labile subunit (ALS) (*2, 7, 9*). This ternary complex of 150 kDa molecular mass is unable to traverse the vasculature walls and acts as a circulating reservoir for IGF's. By this mechanism the half-life of IGF-I is dramatically increased (*52*). The levels of IGFBP-3 are positively regulated by IGF-I. The role of IGFBP-1, in contrast, is less clear. This class of binding proteins is generally less abundant than IGFBP-3, and its levels are negatively regulated by insulin (*2, 7, 9*). Clearly, more work needs to be done in order to understand

how the different IGFBP's achieve a fine-tuned regulation of IGF-I. Important tools in this research could be IGFBP-specific IGF isoforms. It has been demonstrated in animal models that receptor-inactive IGF mutants are able to displace endogenous IGF-I from binding proteins and hereby generate a net IGF-I effect in vivo (*21*, *53*). The same strategy applied to a IGFBP-specific IGF-I mutant should result in displacement of IGF-I from one defined class of binding proteins only while not disturbing the binding equilibria of the other IGFBP classes.

On the basis of our results it seems possible to design IGFBP-specific variants of IGF-I. Combination of several alanine mutations should generate a variant that binds IGFBP-1 very weakly while retaining high-affinity binding of IGFBP-3. The design of IGFBP-1-specific variants that no longer bind to IGFBP-3, however, will likely require more effort. One possible approach would involve the randomization of amino acids at specific positions (*46*, *54*). Again, phage display of IGF-I may prove to be a useful method to achieve this goal.

ACKNOWLEDGMENT

We thank Y. Chen, G. Nakamura, S. Sidhu, and G. Fuh for help with phage protocols; the Genentech oligo synthesis and peptide sequencing groups; S. Schilbach and A. Zhong for DNA sequencing; D. Reifsnyder and M. Gironella for providing purified IGFBP-1 and IGFBP-3; A. Cochran and S. Russell for help with the HPLC purifications; J. Joly for advice on IGF-I expression; C. Wiesmann and M. Arkin for help with the molecular graphics program; and N. Skelton, P. Fielder, and R. Clark for fruitful discussions.

REFERENCES

1. Clark, R. G., and Robinson, I. C. A. F. (1996) *Cytokine Growth Factor Rev. 7*, 65−80.
2. Jones, J. I., and Clemmons, D. R. (1995) *Endocr. Rev. 16*, 3−34.
3. Ullrich, A., Gray, A., Tam, A. W., Yang-Feng, T., Tsubokawa, M., Collins, C., Henzel, W., LeBon, T., Kathuria, S., Chen, E., Jacobs, S., Francke, U., Ramachandran, J., and Fujita-Yamaguchi, Y. (1986) *EMBO J. 5*, 2503−2512.
4. McInnes, C., and Sykes, B. (1998) *Biopolymers 43*, 339−366.
5. Garrett, T. P. J., McKern, N. M., Lou, M., Frenkel, M. J., Bentley, J. D., Lovrecz, G. O., Elleman, T. C., Cosgrove, L. J., and Ward, C. W. (1998) *Nature 394*, 395−399.
6. Baxter, R. C., Binoux, M. A., Clemmons, D. R., Conover, C. A., Drop, S. L. S., Holly, J. M. P., Mohan, S., Oh, Y., and Rosenfeld, R. G. (1998) *Endocrinology 139*, 4036.
7. Bach, L. A., and Rechler, M. M. (1995) *Diabetes Rev. 3*, 38−61.
8. Martin, J. L., and Baxter, R. C. (1994) *Curr. Opin. Endocrinol. Diabetes*, 16−21.
9. Clemmons, D. R. (1997) *Cytokine Growth Factor Rev. 8*, 45−62.
10. Chernausek, S. D., Smith, C. E., Duffin, K. L., Busby, W. H., Wright, G., and Clemmons, D. R. (1995) *J. Biol. Chem. 270*, 11377−11382.
11. Conover, C. A. (1995) *Prog. Growth Factor Res. 6*, 301−309.
12. Kalus, W., Zweckstetter, M., Renner, C., Sanchez, Y., Georgescu, J., Grol, M., Demuth, D., Schumacher, R., Dony, C., Lang, K., and Holak, T. A. (1998) *EMBO J. 17*, 6558−6572.
13. Cooke, R. M., Harvey, T. S., and Campbell, I. D. (1991) *Biochemistry 30*, 5484−5491.
14. Hua, Q. X., Narhi, L., Jia, W. H., Arakawa, T., Rosenfeld, R., Hawkins, N., Miller, J. A., and Weiss, M. A. (1996) *J. Mol. Biol. 259*, 297−313.
15. DeWolf, E., Gill, R., Geddes, S., Pitts, J., Wollmer, A., and Grötzinger, J. (1996) *Protein Sci. 5*, 2193−2202.
16. Terasawa, H., Kohda, D., Hatanaka, H., Nagata, K., Higashihashi, N., Fujiwara, H., Sakano, K., and Inagaki, F. (1994) *EMBO J. 13*, 5590−5597.
17. Torres, A. M., Forbes, B. E., Aplin, S. E., Wallace, J. C., Francis, G. L., and Norton, R. S. (1995) *J. Mol. Biol. 248*, 385−401.
18. Cascieri, M. A., Chicchi, G. G., Applebaum, J., Hayes, N., Green, B. G., and Bayne, M. L. (1988) *Biochemistry 27*, 3229−3233.
19. Bayne, M. L., Applebaum, J., Underwood, D., Chicchi, G. G., Green, B. G., Hayes, N. S., and Cascieri, M. A. (1989) *J. Biol. Chem. 264*, 11004−11008.
20. Bayne, M. L., Applebaum, J., Chichi, G. G., Miller, R. E., and Cascieri, M. A. (1990) *J. Biol. Chem. 265*, 15648−15652.
21. Lowman, H. B., Chen, Y. M., Skelton, N. J., Mortensen, D. L., Tomlinson, E. E., Sadick, M. D., Robinson, I. C. A. F., and Clark, R. G. (1998) *Biochemistry 37*, 8870−8878.
22. Bayne, M. L., Applebaum, J., Chicchi, G. G., Hayes, N. S., Green, B. G., and Cascieri, M. A. (1988) *J. Biol. Chem. 263*, 6233−6239.
23. Bagley, C. J., May, B. L., Szabo, L., McNamara, P. J., Ross, M., Francis, G. L., Ballard, F. J., and Wallace, J. C. (1989) *Biochem. J. 259*, 665−671.
24. Clemmons, D. R., Cascieri, M. A., Camacho-Hubner, C., McCusker, R. H., and Bayne, M. L. (1990) *J. Biol. Chem. 265*, 12210−12216.
25. Clemmons, D. R., Dehoff, M. L., Busby, W. H., Bayne, M. L., and Cascieri, M. A. (1992) *Endocrinology 131*, 890−895.
26. Baxter, R. C., Bayne, M. L., and Cascieri, M. A. (1992) *J. Biol. Chem. 267*, 60−65.
27. Oh, Y., Müller, H. L., Lee, D.-Y., Fielder, P. J., and Rosenfeld, R. G. (1993) *Endocrinology 132*, 1337−1344.
28. Heding, A., Gill, R., Ogawa, Y., De Meyts, P., and Shymko, R. M. (1996) *J. Biol. Chem. 271*, 13948−13952.
29. Jansson, M., Uhlen, M., and Nilsson, B. (1997) *Biochemistry 36*, 4108−4117.
30. Jansson, M., Andersson, G., Uhlen, M., Nilsson, B., and Kördel, J. (1998) *J. Biol. Chem. 273*, 24701−24707.
31. Cunningham, B. C., and Wells, J. A. (1989) *Science 244*, 1081−1085.
32. Wells, J. A. (1991) *Methods Enzymol. 202*, 390−411.
33. Swartz, J. R. (1994) *Method for Producing Polypeptide via Bacterial Fermentation*, U.S. Patent No. 5,342,763.
34. Lowman, H. B., Bass, S. H., Simpson, N., and Wells, J. A. (1991) *Biochemistry 30*, 10832−10838.
35. Kunkel, T. A., Bebenek, K., and McClary, J. (1991) *Methods Enzymol. 204*, 125−139.
36. Wood, W. I., Cachianes, G., Henzel, W. J., Winslow, G. A., Spencer, S. A., Hellmiss, R., Martin, J. L., and Baxter, R. C. (1988) *Mol. Endocrinol. 2*, 1176−1185.
37. Martin, J. L., and Baxter, R. C. (1986) *J. Biol. Chem. 261*, 8754−8760.
38. Mortensen, D. L., Won, W. B., Siu, J., Reifsnyder, D., Gironella, M., Etcheverry, T., and Clark, R. G. (1997) *Endocrinology 138*, 2073−2080.
39. Lowman, H. B. (1998) in *Combinatorial Peptide Library Protocols* (Cabilly, S., Ed.) Vol. 87, pp 249−264, Humana Press, Totowa, NJ.
40. Sambrook, J., Fritsch, E. F., and Maniatis, T. (1989) *Molecular cloning. A laboratory handbook*, Cold Spring Harbor Laboratory Press, Cold Spring Harbor, NY.
41. Joly, J. C., Leung, W. S., and Swartz, J. R. (1998) *Proc. Natl. Acad. Sci. U.S.A. 95*, 2773−2777.
42. Chang, J. Y., and Swartz, J. R. (1993) in *Protein Folding In Vivo and In Vitro* (Cleland, J. L., Ed.) pp 178−188, ACS Symposium Series, American Chemical Society, Washington, DC.
43. Hober, S., Forsberg, G., Palm, G., Hartmanis, M., and Nilsson, B. (1992) *Biochemistry 31*, 1749−1756.

44. Miller, J. A., Owers Narhi, L., Hua, Q.-X., Rosenfeld, R., Arakawa, T., Rohde, M., Prestrelski, S., Lauren, S., Stoney, K. S., Tsai, L., and Weiss, M. A. (1993) *Biochemistry 32*, 5203−5213.
45. Bass, S., Green, R., and Wells, J. A. (1990) *Proteins 8*, 309−314.
46. Cunningham, B. C., Lowe, D. G., Li, B., Bennet, B. D., and Wells, J. A. (1994) *EMBO J. 13*, 2508−2515.
47. Di Cera, E. (1998) *Chem. Rev. 98*, 1563−1591.
48. Bogan, A. A., and Thorn, K. S. (1998) *J. Mol. Biol. 280*, 1−9.
49. Clackson, T., and Wells, J. A. (1995) *Science 267*, 383−386.
50. Kelley, R. F., Costas, K. E., O'Connell, M. P., and Lazarus, R. A. (1995) *Biochemistry 34*, 10383−10392.
51. Mañes, S., Kremer, L., Albar, J. P., Mark, C., Llopis, R., and Martínez, C. (1997) *Endocrinology 138*, 905−915.
52. Simpson, H. L., Umpleby, A. M., and Russell-Jones, D. L. (1998) *Growth Horm. IGF Res. 8*, 83−95.
53. Loddick, S. A., Liu, X.-J., Lu, Z.-X., Liu, C., Behan, D. P., Chalmers, D. C., Foster, A. C., Vale, W. W., Ling, N., and De Souza, E. B. (1998) *Proc. Natl. Acad. Sci. U.S.A. 95*, 1894−1898.
54. Lowman, H. B., and Wells, J. A. (1993) *J. Mol. Biol. 243*, 564−578.

BI990089P